This article has been accepted for publication in a future issue of this journal, but has not been fully edited. Content may change prior to final publication. Citation information: DOI 10.1109/TPWRD.2014.2357471, IEEE Transactions on Power Delivery

A Control Method for Inverter-Based Islanded Microgrids Based on V-I Droop Characteristics

Mohammad S. Golsorkhi, *Student Member, IEEE* and Dylan.D.C. Lu, *Senior Member, IEEE*

***Abstract*—Microgrids performance and stability mostly depend on power flow control strategy. In order to allow for a coordinated control while maintaining a reliable operation, decentralized control methods based on P and Q droop characteristics have been utilized. Inherently, the power droop control methods have slow dynamics. In this paper, a novel control method based on V-I characteristics is introduced to exploit the flexibility and fast dynamics of the inverter-based Distributed Energy Resources (DERs). In the proposed method, the direct and quadrature axis voltage components are drooped with the corresponding currents according to a piecewise linear droop function. Eigenvalue analysis of a sample microgrid shows that the proposed method features faster dynamics and improved damping compared to the conventional droop scheme. Simulation results are presented to verify the efficacy of the proposed method.**

***Index Terms*— microgrids, distributed energy resource (DER), control, inverter, droop, power sharing.**

I. Introduction

With the increasing penetration of distributed energy resources (DERs) in power grids, new challenges on performance, stability and control have been arisen. One way to deal with these issues is to take a system approach, which views DERs and associated loads as a subsystem or a "microgrid" [1]. The microgrid concept favors a coordinated control, in which DER units can cooperate to deliver a high quality and reliable energy to consumers. In the recent years, several research works have been conducted to realize a high performance, coordinated microgrid control strategy [2]-[21]. From the implementation viewpoint, they can be divided into two main categories: centralized and decentralized control methods [2]. The centralized control methods rely on a high-bandwidth communication link to transfer feedback and control signals between DERs and a centralized controller [6]. Besides the additional cost of the communication system, centralized controllers are less reliable because any communication interruption might cause instability. Therefore, decentralized control methods are more practical.

The decentralized control methods utilize P-f and Q-E droop characteristics to control active and reactive power flow in microgrids, respectively. The P-f / Q-E droop scheme is based on highly inductive networks, in which active and reactive power flow equations can be decoupled. Moreover, it is characterized by slow dynamics [7] and frequency and voltage drifts with the load change [8]. The aforementioned characteristics are in accordance with the high X/R ratio of the network impedance and large inertia of turbine-governor systems in conventional power systems. Moreover, since the variations of aggregated loads in high voltage systems are smooth, the resulting frequency drifts can be compensated by a low bandwidth secondary controller. In microgrids, however, lines impedances are mostly resistive, DERs have a small inertia and frequent step load changes might occur.

Unlike the conventional power systems, the X/R ratio in microgrids is not large. Therefore, the active and reactive power flows are highly coupled and dependent on both δ and E. That results in poor performance of the conventional droop method, which is based on decoupled P-f and Q-E control. To overcome this issue, different controllers are proposed [9]-[11]. In [9] virtual PQ method has been used to simulate an inductive system, where the P-f and Q-E droops are decoupled. In [10] a virtual reactance is introduced at the inverter output to increase the X/R ratio. In [11] a virtual resistance is introduced at the inverter output to make the system prominently resistive, in which P and Q can be controlled by drooping E and f, respectively.

The P-f/Q-E droop scheme suffers from power quality issues including frequency and voltage deviations. Frequency deviations can be eliminated by utilizing P-δ droop instead of the P-f droop [12]. In that method, global positioning system (GPS) is utilized as a time reference, to synchronize DER units. This allows even power sharing by directly controlling DERs power angle (δ). In [13] an adaptive voltage droop method has been introduced to improve voltage regulation at point of common coupling (PCC) and alleviate the coupling between P and Q droop controllers.

The power droop control methods are intrinsically low bandwidth controllers with slow dynamics. Moreover, increasing droop coefficients results in a degraded dynamic response and ultimately instability [14]. The stability of the P-δ droop method can be improved by adding a supplementary controller, which controls the voltage amplitude based on the variations of P [15]. Ref [16] has replaced the linear supplementary controller by a nonlinear controller to maintain system stability even in case of large signal disturbances. In [14] an adaptive derivative term has been added to the P and Q droop controllers to decrease current overshoot and improve stability.

In [17] an adaptive feed-forward control scheme is proposed to eliminate the dependency of microgrid performance and stability on droop coefficient and load dynamics. The scheme reshapes the conventional droop characteristics by injecting two supplementary control signals in the voltage control loop. However, the performance of the method is dependent on an identification mechanism, which is

M.S. Golsorkhi Author, Jr., is with The School of Electrical and Information Engineering, The University of Sydney, Sydney, Australia.(e-mail: mohammad.golsorkhiesfahani@sydney.edu.a).

D.D.C. Lu Author, is with The School of Electrical and Information Engineering, The University of Sydney, Sydney, Australia.(e-mail: dylan.lu@sydney.edu.a).

This article has been accepted for publication in a future issue of this journal, but has not been fully edited. Content may change prior to final publication. Citation information: DOI 10.1109/TPWRD.2014.2357471, IEEE Transactions on Power Delivery

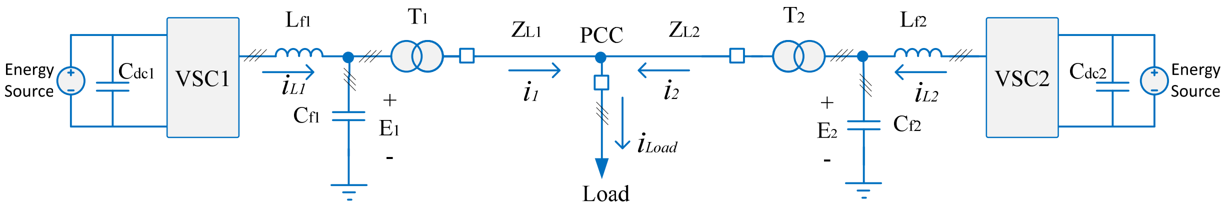

Fig. 1. Microgrid model

used to calculate feed-forward gain. Ref [18] has improved the method by using a gain scheduled scheme.

The existing communication-less microgrid control methods utilize P-f(δ) and Q-E or P-E and Q-f(δ) droop characteristics. This paper proposes an alternative approach, in which the problem of power sharing is simplified to current sharing. In this method, DERs are coordinated by adjusting the inverter voltage as a function of current. This change simplifies the nonlinear control problem of P/Q sharing to linear problem of current sharing. In addition, with the inherent delay of P/Q measurement eliminated, the controller reacts quickly subsequent to load changes. Since the inverter voltage variations are small, the objectives of P and Q sharing are satisfied. By applying the method to a microgrid, it is shown that the system dynamic response depends on droop function. A piecewise linear droop function is adopted to increase damping as well as power sharing accuracy at high loading conditions, when the DERs are vulnerable to overload.

The rest of the paper is organized, as follows. The proposed method is formulated in section II. In section III, the interaction of the droop controller with the internal voltage-current control loops is investigated by eigenvalue analysis. Simulation results based on CIGRE benchmark microgrid are demonstrated in section IV to verify the effectiveness of the proposed method.

II. Proposed Control Method

Droop-based control methods utilize some electrical parameters such as frequency and voltage as a signal for coordination of local controllers (LCs) in a microgrid. In order to allow for constant frequency operation, a GPS signal, which is a pulse train with period of 1s, is used to synchronize LCs [12]. With the LCs synchronized, all electrical parameters of the microgrid can be referred to a common synchronous reference frame. In this context, voltage can be used as a droop variable, either in polar (E and δ) or rectangular (E_q and E_d) coordinates. The former, which has been used in P-δ/Q-E droop method [12], requires linearization of power flow equations, whereas the latter does not. In this paper, the LCs are coordinated by drooping E_q and E_d with i_q and i_d. By selecting an appropriate droop function, i_q and i_d can be shared evenly between the DERs. Assuming $V_q\approx 1$ and $V_d\approx 0$, i_q and i_d approximately represent the active and reactive power, respectively. Therefore, even power sharing is guaranteed.

Fig. 1 illustrates a simple microgrid consisting of two DERs and one load. The DERs are assumed to be dispatchable, i.e., capable of producing active power on demand. Each DER consists of an energy source, a voltage source converter (VSC) followed by an LC filter and an isolation transformer. The DERs are connected to the PCC via low voltage cables. The isolation transformer and low voltage cables corresponding to DER$_x$ (x=1 or 2) have impedances of $Z_{Tx}=R_{Tx}+j\omega L_{Tx}$ and $Z_{Lx}=R_{Lx}+j\omega L_{Lx}$, in which $\omega=100\pi$ is the system angular frequency.

The system parameters can be represented in a global synchronous rotating reference frame, as shown in Fig. 2. All DERs are synchronized with the global reference frame using the GPS signal. The interaction of DERs is described by KVL and KCL equations, as follows:

$$L_1 p\begin{bmatrix} i_{1q} \\ i_{1d} \end{bmatrix} = \begin{bmatrix} E_{1q} \\ E_{1d} \end{bmatrix} - \begin{bmatrix} V_q^{pcc} \\ V_d^{pcc} \end{bmatrix} - \begin{bmatrix} R_{T1}+R_{L1} & X_{T1}+X_{L1} \\ -X_{T1}-X_{L1} & R_{T1}+R_{L1} \end{bmatrix}\begin{bmatrix} i_{1q} \\ i_{1d} \end{bmatrix} \quad (1)$$

$$L_2 p\begin{bmatrix} i_{2q} \\ i_{2d} \end{bmatrix} = \begin{bmatrix} E_{2q} \\ E_{2d} \end{bmatrix} - \begin{bmatrix} V_q^{pcc} \\ V_d^{pcc} \end{bmatrix} - \begin{bmatrix} R_{T2}+R_{L2} & X_{T2}+X_{L2} \\ -X_{T2}-X_{L2} & R_{T2}+R_{L2} \end{bmatrix}\begin{bmatrix} i_{2q} \\ i_{2d} \end{bmatrix} \quad (2)$$

$$\begin{bmatrix} i_{1q} \\ i_{1d} \end{bmatrix} + \begin{bmatrix} i_{2q} \\ i_{2d} \end{bmatrix} = \begin{bmatrix} i_q^{Load} \\ i_d^{Load} \end{bmatrix} \quad (3)$$

in which $X_{Tx}=\omega L_{Lx}$, $X_{Lx}=\omega L_{Lx}$ and $L_x=L_{Tx}+L_{Lx}$ and prefix "p" denotes derivative.

The PCC voltage can be eliminated from (1) and (2) by subtraction, as follows:

$$L_1 p\begin{bmatrix} i_{1q} \\ i_{1d} \end{bmatrix} - L_2 p\begin{bmatrix} i_{2q} \\ i_{2d} \end{bmatrix} = \begin{bmatrix} E_{1q} \\ E_{1d} \end{bmatrix} - \begin{bmatrix} E_{2q} \\ E_{2d} \end{bmatrix} - \left[Z_1\right]\begin{bmatrix} i_{1q} \\ i_{1d} \end{bmatrix} + \left[Z_2\right]\begin{bmatrix} i_{1q} \\ i_{1d} \end{bmatrix} \quad (4)$$

In which, $\left[Z_x\right] = \begin{bmatrix} R_{Tx}+R_{Lx} & X_{Tx}+X_{Lx} \\ -X_{Tx}-X_{Lx} & R_{Tx}+R_{Lx} \end{bmatrix}$.

Equation (4) shows that i_q and i_d are related to the difference between the inverters voltages through linear differential equations. Therefore, it is possible to control the load sharing between the inverters by adjusting the inverters voltages. In order to achieve the aim of even current sharing between the DERs, the reference voltage of the inverters are determined based on the following droop control law:

$$\begin{bmatrix} E_{xq}^* \\ E_{xd}^* \end{bmatrix} = \begin{bmatrix} E_0 \\ 0 \end{bmatrix} - \begin{bmatrix} f_x\left(i_{xq}, i_{xd}\right) \\ g_x\left(i_{xq}, i_{xd}\right) \end{bmatrix} \quad (5)$$

where, E_0 is no load voltage, and f and g are arbitrary functions of the current. A cascaded voltage-current regulator is used to keep track of the reference voltage. The time constant of the cascaded controller is in the order of milliseconds, thanks to the fast dynamics of the inverter and the large resonance frequency of the LC filter. In order to simplify analysis, the dynamics of voltage regulator are not considered in this section. The behavior of the proposed control considering the dynamics of the voltage regulator as well as the LC filter is investigated in section III.

Assuming $E=E^*$ and substituting (5) into (4) it can be shown that the ratio of the DER currents (i_{1d}/i_{2d} and i_{1q}/i_{2q}) is dependent on the functions f and g as well as the system parameters. In order to eliminate the adverse effect of

This article has been accepted for publication in a future issue of this journal, but has not been fully edited. Content may change prior to final publication. Citation information: DOI 10.1109/TPWRD.2014.2357471, IEEE Transactions on Power Delivery

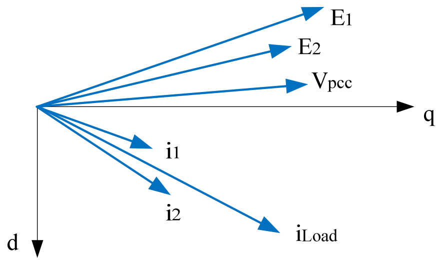

Fig. 2. Representation of system parameters in the gloal reference frame

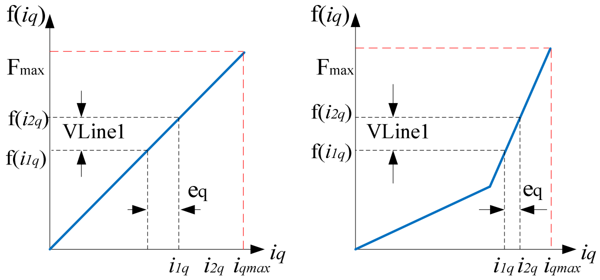

(a) (b)

Fig. 3. Droop function: a) linear, b) piece-wise linear

transformer impedance on the power sharing and voltage regulation, compensating terms are added to the control law, as follows:

$$\begin{bmatrix} E_{xq}^{*} \\ E_{xd}^{*} \end{bmatrix} = \begin{bmatrix} E_0 \\ 0 \end{bmatrix} + \begin{bmatrix} R_{Tx} & X_{Tx} \\ -X_{Tx} & R_{Tx} \end{bmatrix} \begin{bmatrix} i_{xq} \\ i_{xd} \end{bmatrix} - \begin{bmatrix} f_x\left(i_{xq}, i_{xd}\right) \\ g_x\left(i_{xq}, i_{xd}\right) \end{bmatrix} \quad (6)$$

The droop functions can be chosen as a linear combination of i_q and i_d, as follows:

$$\begin{bmatrix} f_x \\ g_x \end{bmatrix} = \begin{bmatrix} m_x & l_x \\ -k_x & n_x \end{bmatrix} \begin{bmatrix} i_{xq} \\ i_{xd} \end{bmatrix} \quad (7)$$

in which, the droop coefficients (m, n, l and k) are selected inversely proportional to the DERs ratings. Substituting (7) into (6) and using (4), the system dynamics can be written, as follows:

$$\begin{aligned} & L_1 p \begin{bmatrix} i_{1q} \\ i_{1d} \end{bmatrix} - L_2 p \begin{bmatrix} i_{2q} \\ i_{2d} \end{bmatrix} = \\ & \begin{bmatrix} -R_{L1} - m_1 & -X_{L1} - l_1 \\ X_{L1} + k_1 & -R_{L1} - n_1 \end{bmatrix} \begin{bmatrix} i_{1q} \\ i_{1d} \end{bmatrix} - \begin{bmatrix} -R_{L2} - m_2 & -X_{L2} - l_2 \\ X_{L2} + k_2 & -R_{L2} - n_2 \end{bmatrix} \begin{bmatrix} i_{2q} \\ i_{2d} \end{bmatrix} \end{aligned} \quad (8)$$

Equation (8) implies that steady state current sharing is dependent on the droop coefficients and line impedances. It is worthwhile to mention that low voltage distribution systems, on which this paper is focused, cover small regions hence lines are of short length and small impedance (in the order of 0.01-0.02pu). Therefore, even power sharing can be achieved by selecting appropriate droop coefficients.

In order to derive a compact representation for the system, it can be assumed that the pu transformer and line impedances match ($Z_{L1}^{pu} = Z_{L2}^{pu}$ and $Z_{T1}^{pu} = Z_{T2}^{pu}$). In this case, steady-state current sharing error is zero and (8) can be simplified to the following equation:

$$L_1^{pu} p \begin{bmatrix} e_q \\ e_d \end{bmatrix} = \begin{bmatrix} -R_{L1}^{pu} - m_1^{pu} & -X_{L1}^{pu} - l_1^{pu} \\ X_{L1}^{pu} + k_1^{pu} & -R_{L1}^{pu} - n_1^{pu} \end{bmatrix} \begin{bmatrix} e_q \\ e_d \end{bmatrix} \quad (9)$$

where, $e = i_1^{pu} - i_2^{pu}$ represents the current sharing error. Since line impedances are small compared to the droop coefficients, the system dynamic response is mostly dependent on the coefficients. Two extreme cases are considered here. In the first case, the diagonal coefficients (m and n) are set to zero to have i_q-E_d /i_d-E_q droop characteristics. It is noteworthy to mention the similarity of these characteristics with the conventional droop (P-δ/Q-E). That choice leads to an under-damped response, with damping ratio decreasing with the increase of the coefficients. In the second case, the off-diagonal elements are set to zero. With this choice, the q and d components of the current are approximately decoupled thanks to the small X/R ratio of the lines. Moreover, the increase of coefficients m and n improves both damping and steady state current sharing. However, the droop action causes PCC voltage drop. Therefore, the coefficients should be chosen such that the PCC voltage is in the permissible range.

From (8) it can be inferred that steady-state current sharing error is dependent on the mismatch of the line voltage drops and increases with the load rise. On the other hand, the system is more vulnerable under heavy loading conditions, as the DER output currents are strictly limited by the current rating of the inverters' switches. In order to decrease the current sharing error and improve the damping under heavy loading conditions, a piece-wise linear droop function is adopted. Therefore, the droop control law is defined as follows:

$$\begin{bmatrix} E_{xq}^{*} \\ E_{xd}^{*} \end{bmatrix} = \begin{bmatrix} E_0 \\ 0 \end{bmatrix} + \begin{bmatrix} R_{Tx} & X_{Tx} \\ -X_{Tx} & R_{Tx} \end{bmatrix} i_{xqd} - \begin{bmatrix} m_x f\left(i_{xq}\right) \\ n_x f\left(i_{xd}\right) \end{bmatrix} \quad (10)$$

Fig. 3 illustrates a comparison between steady-state error of linear and piece-wise linear droop functions. As for representation, the DER ratings are assumed to be equal and the line 2 impedance is assumed to be zero.

Having i_{1q} known, f(i_{2q}) is calculated, as follows:

$$f(i_{2q}) = f(i_{1q}) + \begin{bmatrix} R_{L1} & X_{L1} \end{bmatrix} i_{1qd} \quad (11)$$

It is observed that while the maximum of both droop functions are equal, the current sharing error is much smaller for the piece-wise linear droop. Moreover, the higher droop slope at high loading conditions corresponds to an improved dynamic response.

In order to achieve the optimum performance, the function f is designed by solving the following optimization problem:

$$\begin{aligned} \min \quad & Cf = C_1 \overline{e}_{low} + C_2 \overline{e}_{medium} + C_3 \overline{e}_{high}, \\ st. \quad & f(0) = 0, \\ & f(1) = 1, \end{aligned}$$

where, $\overline{e}_{low}$, $\overline{e}_{medium}$ and $\overline{e}_{high}$ are average current sharing error at low ($0<i<0.5$pu), medium ($0.5\text{pu}<i<0.7$pu) and high ($i>0.7$pu) loading conditions, respectively. In order to emphasize vulnerability of the system at high loading conditions, the weights C_1, C_2 and C_3 are set to 1, 2 and 8, respectively. The objective is to find the slope of the function at different loading conditions, to minimize the cost function.

TABLE I. PIECE-WISE LINEAR FUNCTION F

i (pu)	-1	-0.7	-0.5	0.5	0.7	*1*
f (i)	-1	-0.35	-0.15	0.15	0.35	*1*

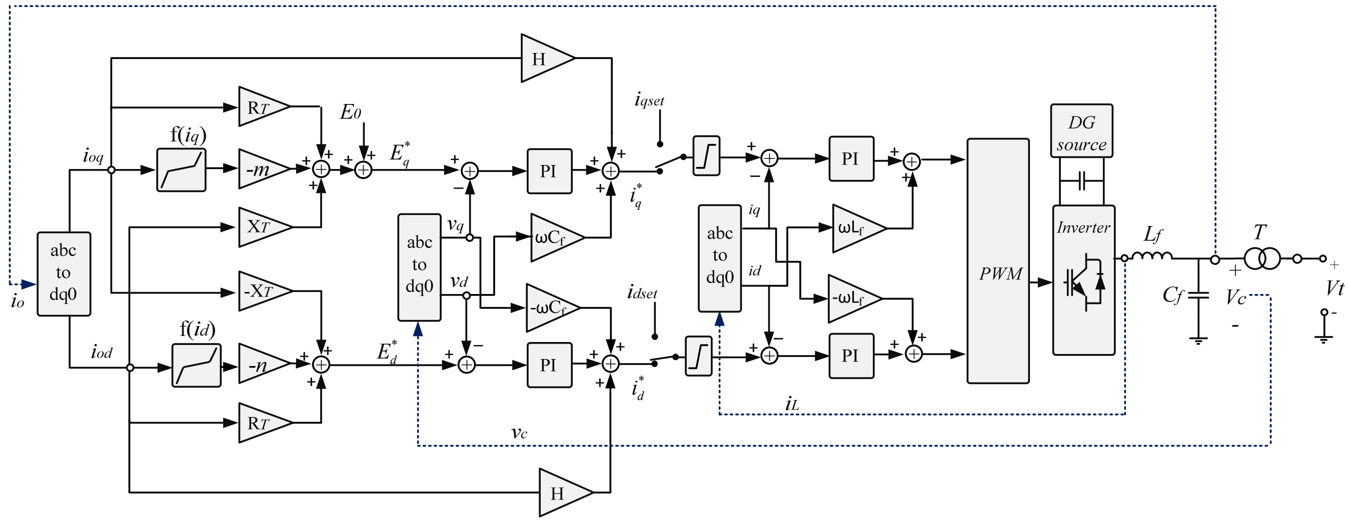

Fig. 4. Proposed controller schematic

The optimization problem is solved numerically. The resulting slopes are 0.3, 1 and 2.16 for low, medium and high loading conditions, respectively. The function f is then extended for negative currents and represented as a look-up table, as shown in table I.

The proposed controller is illustrated in Fig. 4. The droop controller calculates the inverter reference voltage according to (10). The reference voltage is then fed to a cascaded PI controller consisting of voltage and current feedback loops and a current feed-forward loop. A current limiter along with an anti-windup feedback is used in the voltage controller to protect the inverter from over-current during transient or fault conditions. The DER operating mode is selected by an automatic switch. The current controller output is fed to the PWM module to control the switching duty cycle.

From the implementation standpoint, the proposed controller is quite similar to the conventional P-f/Q-E droop methods, except utilizing the output transformer impedance in the droop control law. The effect of the impedance variations on the controller performance is discussed in section IV.

III. SMALL-SIGNAL ANALYSIS OF THE MICROGRID

In this section, small-signal behavior of the proposed control considering the dynamics of the cascaded voltage regulator as well as the LC filter is investigated. The proposed controller is applied to the microgrid of Fig. 1 and the system is modeled in the synchronous rotating reference frame. The model is formulated in state-space form with 20 independent states, including filter capacitors voltages, filter inductors currents, voltage and current regulator integrators, DER output currents and load voltage. The system is linearized around the operating point which is calculated by time-domain simulation. The dynamic response and stability is then investigated by eigenvalue analysis using MATLAB Control Design Toolbox.

The system parameters are listed in table II. Each DER has a power rating of 30kW. Lines 1 and 2 are standard low voltage XLPE-16 overhead cables with lengths of 35m and 105m, respectively. The system load is set to 50kW at 0.7 PF lagging to replicate heavy loading conditions. According to EN 50160, the 10 minute rms voltage of low voltage networks should remain in the range of 90% to 110% of the nominal value [19]. With the power electronic controllers, the voltage can be maintained in a narrow range. In this paper, the permissible voltage deviation at the DERs terminals is $\pm 4\%$. In order to maintain the voltage within the permissible range, the q axis droop coefficient (*m*) is set to 0.08 and E_0 is set to 1.04pu. Therefore, the voltage remains within 0.96pu and 1.04pu.The system eigenvalues are then calculated for different values of d axis droop coefficient (*n*).

Fig. 5 depicts the loci of the dominant eigenvalues with n increasing from 0.01 to 0.15. As n is increased from 0.01 to 0.06, the dominant eigenvalue (number 1) quickly shift away from the imaginary axis, but the high frequency eigenvalues slowly move towards the imaginary axis. At n=0.06, the eigenvalue number 2, which moves slowly with increase of n, becomes dominant. This implies a trade-off between power sharing accuracy and dynamic response. However, as n is varied in the range (0.06, 0.15) the high frequency eigenvalues remain far away from the dominant eigenvalue, the real part of which is smaller than -2π*50 *rad/s*. Therefore, the droop controller has a time constant of less than 1 cycle, i.e., it reacts to load changes in the first cycle after the disturbance. The fast coordinated reaction of LCs ensures that the load change is

TABLE II. SYSTEM PARAMETERS

Discription	Parameter	Value	Unit
System parameters	f_{rated}	50	Hz
	V_{Lrated}	400	V
DER 1 and 2 rating	P	30	kW
	S	45	kVA
Filter impedance	$Z_f=R_f+j\omega L_f$	0.05+j0.16	pu
Filter capacitor Reactance	X_C	15.3	pu
DER1 and 2 Transformers' impedances	Z_{T1}	0.03 + j0.09	pu
	Z_{T2}	0.02 + j0.06	pu
Line 1 length		35	m
Line 2 length		105	m
Inner loop PI controller parameters	k_{pi}	10	-
	k_{ii}	15000	-
Outer loop PI controller parameters	k_{pv}	0.025	-
	k_{iv}	200	-
Feed-forward gain	H	0.7	-

This article has been accepted for publication in a future issue of this journal, but has not been fully edited. Content may change prior to final publication. Citation information: DOI 10.1109/TPWRD.2014.2357471, IEEE Transactions on Power Delivery

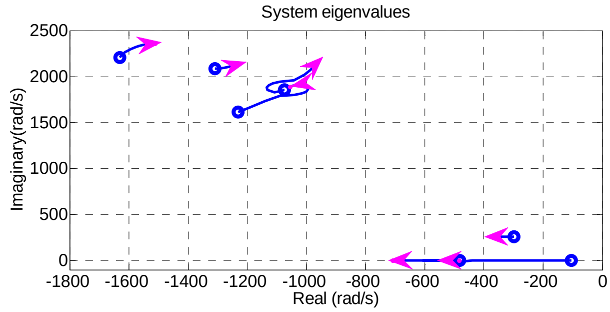

Fig. 5. Eigenvalue loci of the proposed method

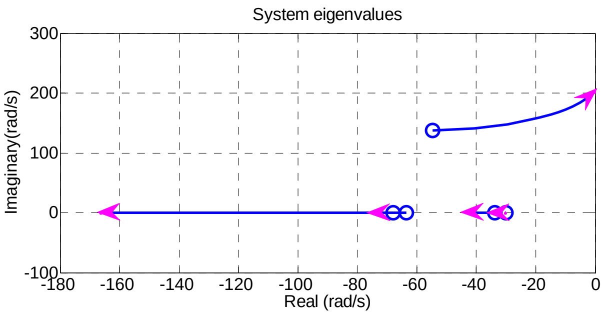

Fig. 6. Eigenvalue loci of conventional P-δ droop method

picked up by all DERs, hence preventing current overshoot. It is worthwhile to mention that the loci of the system eigenvalues with variation of m are similar to Fig. 5 and are not shown here for conciseness.

As for comparison, the loci of the dominant eigenvalues with conventional P-δ/Q-E droop are shown in Fig. 6. The Q-E droop coefficient is set to 0.08 and the P-δ droop coefficient is varied from 0.05 to 0.5. It can be observed that as the droop coefficient is increased, the dominant eigenvalues shift towards the imaginary axis until the system becomes unstable. This behavior is consistent with the mathematical analysis of section 2. Similar results have been reported for P-f/Q-E droop control method [14].

IV. Simulation Results

In order to verify the efficacy of the proposed control method, it is applied to the CIGRE benchmark microgrid proposed in [20]. The benchmark schematic diagram is depicted in Fig. 7. It simulates common low voltage distribution feeders with variety of load types. Five DER units are integrated into the feeder to provide an uninterruptable energy supply. The overhead lines and loads parameters are shown on the diagram. The load power factor is set to 0.7 to replicate worst case conditions in a residential area. The DERs 1 and 2 have the same parameters as listed in table II. The rest of the parameters are shown in table III. Droop coefficients m and n are set to 0.08 and 0.15, respectively. While m is limited by the permissible voltage deviations ($\pm 4\%$), n is selected based on a trade-off between dynamic response and Q sharing accuracy.

The benchmark microgrid is modeled in MATLAB/Simulink and time-domain simulations are conducted to study the system dynamic response to step load change and fault triggered islanding scenarios.

The first scenario is a step load change at the apartment building. The apartment load is raised from 13.5kW to 45 kW

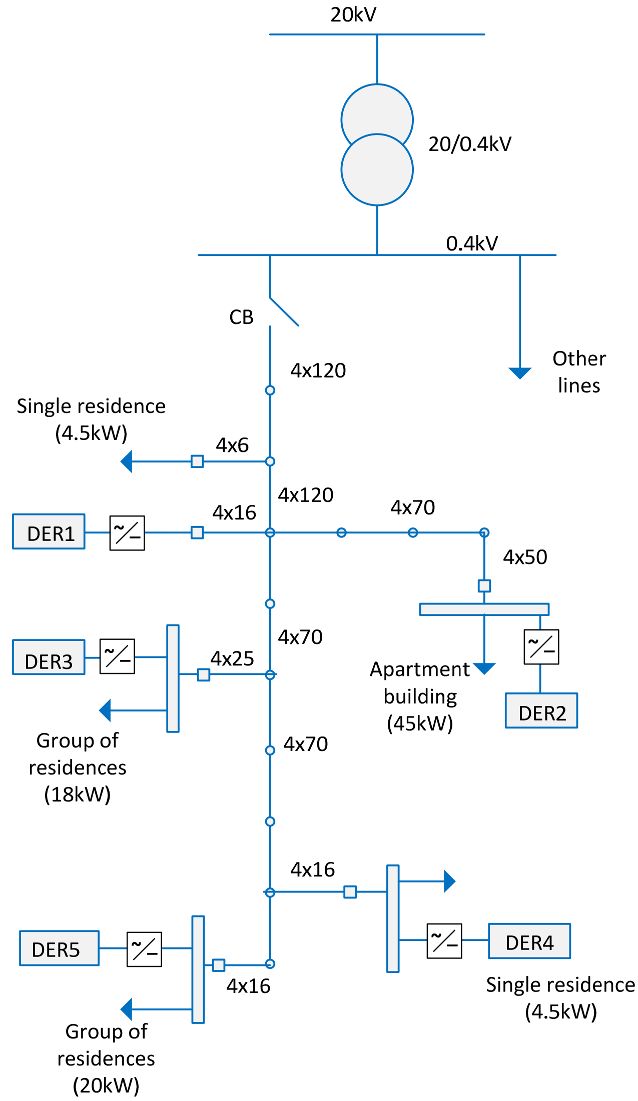

Fig. 7. Benchmark microgrid

at 0.2s and then reduced back to 13.5kW at 0.7s. The DERs active and reactive powers, output currents and voltages with the conventional P-δ droop method are illustrated in Fig.8-(a) to (d), respectively. It is worthwhile to mention that the system response with the P-f droop is quite similar to the P-δ droop and is not shown here for conciseness. It is observed that the system response undergoes several oscillations until settling to the steady-state conditions. Moreover, the reactive power

TABLE III. Benchmark Parameters

Discription	Parameter	Value	Unit
DER 3-5 ratings	S	22.5	kVA
	P	15	kW
DERs Transformers' impedances	Z_{T3}	0.025 + j0.075	pu
	Z_{T4}	0.02 + j0.06	pu
	Z_{T5}	0.03 + j0.09	pu
Proposed method droop coefficients	m	0.08	-
	n	0.15	-
Conventional droop coefficients	k_p	0.1	-
	k_q	0.04	-

This article has been accepted for publication in a future issue of this journal, but has not been fully edited. Content may change prior to final publication. Citation information: DOI 10.1109/TPWRD.2014.2357471, IEEE Transactions on Power Delivery

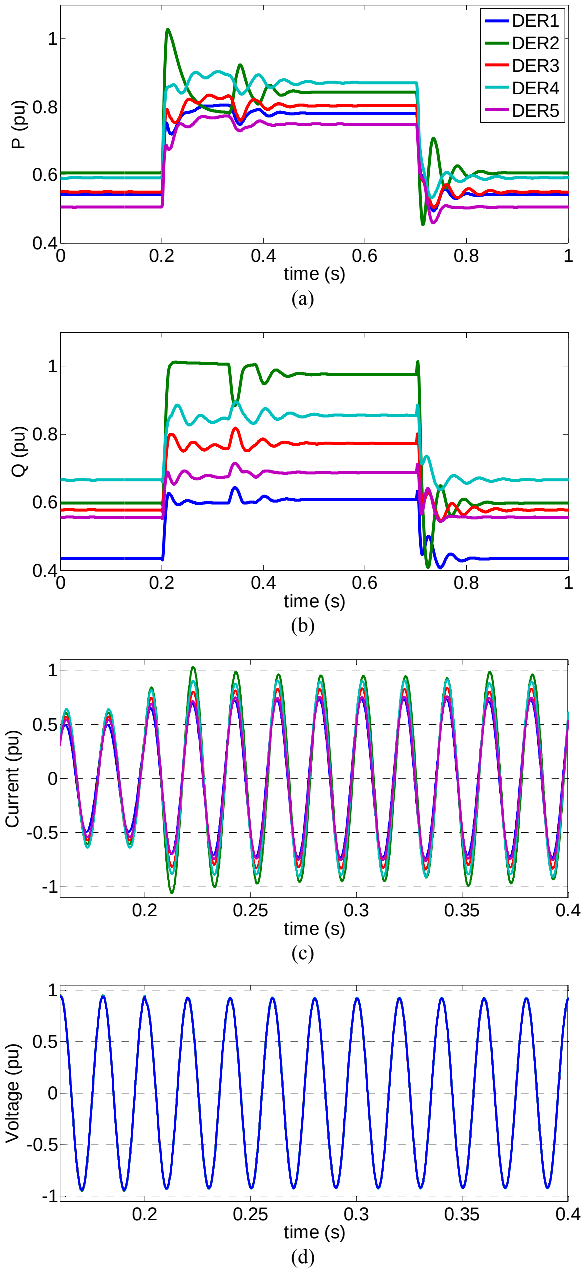

Fig. 8. System response due to a step load change in the apartment building with the conventional droop control method: a) active power, b) reactive power c) current and d) voltage of different DER units

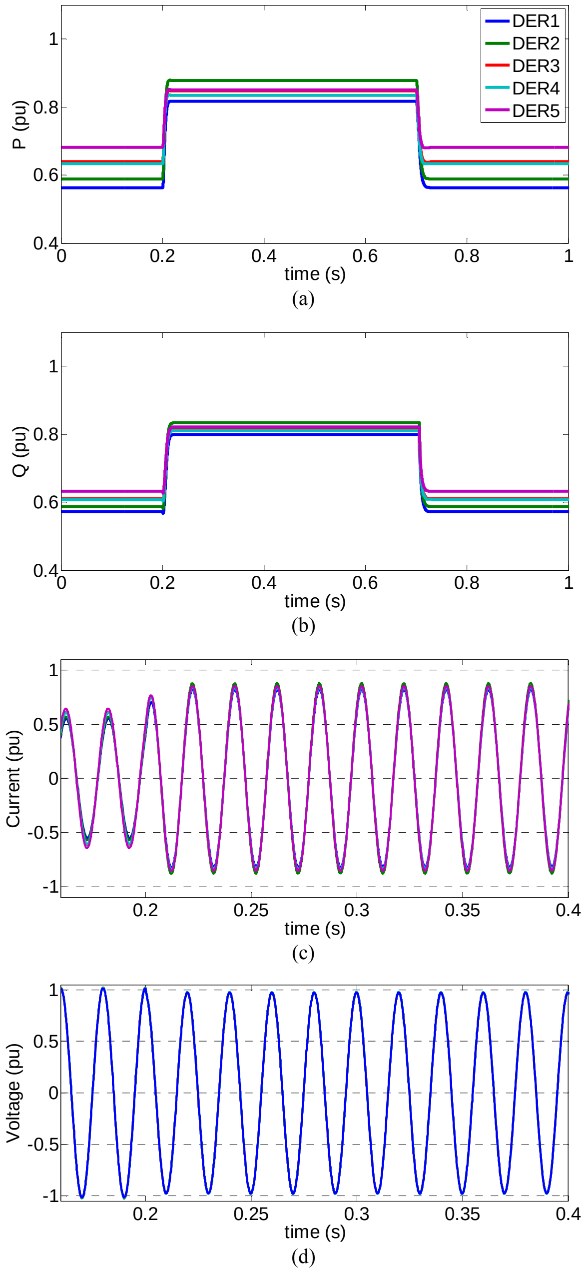

Fig. 9. System response due to a step load change in the apartment building with the proposed control method: a) active power, b) reactive power c) current and d) voltage of different DER units

sharing is quite poor due to the small Q-E droop coefficient and unequal pu impedance of DERs transformers. The current sharing is hence poor and the output current of DER_2, which is located close to the apartment building, rises up to 1.03 in the first cycle after the disturbance. This overshoot might stress the inverter switches and threat the system security. The voltages are almost equal due to the low line impedances. The voltage drops from 0.94pu to 0.92pu after the load increase. The poor voltage regulation is caused by a combination of the Q-E droop control action and the voltage drop on the DER transformers.

The system response with the proposed method is depicted in Fig. 9. With a time constant of less than 1 cycle, all LCs react to the load increase in the first cycle after the disturbance. Therefore, the DERs currents rise smoothly and without overshoot. The maximum current of DER_2 is 0.88pu, which is 0.15pu lower than the conventional method case. The active and reactive powers also rise smoothly. Steady-state errors of active and reactive power sharing are initially within $\pm 6\%$ and $\pm 3\%$, respectively. The errors reduce to half after the load increase, ensuring the DERs will not be overloaded during heavy loading conditions. With the load increase the voltage decreases from 1.02pu to 0.98pu, which is in the permissible range ($\pm 4\%$).

In the second scenario, the microgrid is initially operating in the grid connected mode, until a fault occurs at the

This article has been accepted for publication in a future issue of this journal, but has not been fully edited. Content may change prior to final publication. Citation information: DOI 10.1109/TPWRD.2014.2357471, IEEE Transactions on Power Delivery

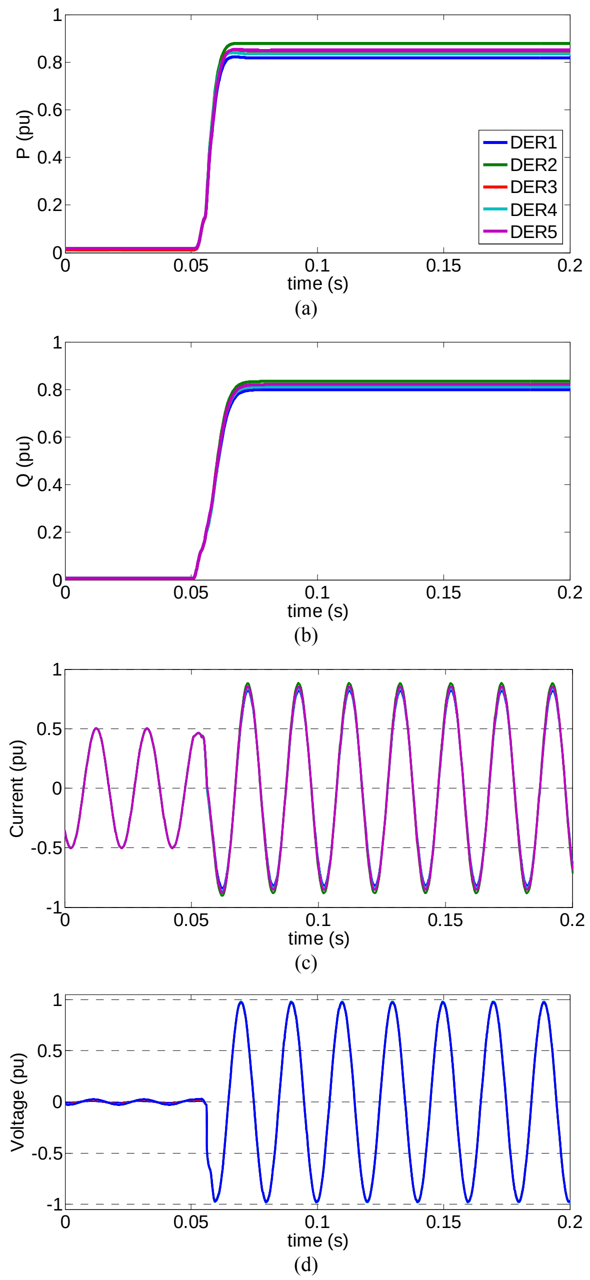

Fig. 10. System response due to a fault triggered islanding with the proposed control method: a) active power, b) reactive power c) current and d) voltage of different DER units

upstream network. The main circuit breaker then opens and the microgrid is switched to the islanding mode. The simulation results are illustrated in Fig. 10. During the fault conditions, the voltage is nearly zero so are the active and reactive powers. At t=0.05 the microgrid is islanded and the LCs are switched to the droop control mode. Subsequently, the voltage is raised by the coordinated action of the LCs. It is observed that the controller responds equally well to islanding, which is a large signal disturbance.

As described in Section II, the transformer impedance is utilized in the droop control law to compensate the transformer voltage drop. The impedance might change slightly as a result of temperature variations or aging. In order to evaluate the sensitivity of the proposed method to the transformer parameters variations, the impedance of DER_1 transformer is changed in the range of 90% to 110% of its original value. Scenario 1 is repeated for several different values of the impedance and power sharing error for each DER is calculated as follows:

$$P_{error,x} = \frac{P_x}{P_{rated,x}} - \frac{\sum_{i=1}^{5} P_i}{\sum_{i=1}^{5} P_{i,rated}} \tag{12}$$

The reactive power and current sharing errors are calculated similarly. The maximum power and current sharing errors for the proposed method (denoted as P) along with the conventional method (denoted as C) are listed in table IV. It is observed that although the variations of the transformer parameters results in an increase of errors, they are still smaller than those of the conventional droop method.

TABLE IV. POWER AND CURRENT SHARING ERROR WITH ALTERED TRANSFORMER PARAMETERS

Discription	Initial load		Increased Load	
	P	C	P	C
Maximum P sharing error	7.9%	9.2%	5.4%	19.8%
Maximum Q sharing error	3.2%	13.5%	2.3%	21.5%
Maximum current sharing error	4.9%	10.1%	3.9%	20.1%

Simulation results show the effectiveness of the proposed method in improving the system dynamic response hence alleviating the current overshoots and stress on the inverter switches. The steady state error of active power sharing can be justified by the fact that perfect even sharing of P is usually neither economic nor necessary. Nonzero error might only result in some DERs reaching the maximum P limit, after which their active power is kept constant.

V. CONCLUSIONS

Microgrids provide a context for facilitating the integration of renewable energy resources in low voltage networks while delivering a high quality and reliable energy to consumers. However, low inertia, strict current limits and small size of inverter-based DERs on one hand and large step load changes on the other hand make microgrids vulnerable to power quality and stability issues.

The authors suggest that dynamic and stability of microgrids can be improved significantly by designing a droop control scheme in accordance with the characteristics of inverter-based DERs, i.e., low inertia and strict current limits. In this paper, a new coordinated control method based on V-I droop characteristic is proposed to fulfill the aforementioned aims. In order to improve power sharing accuracy at high loading conditions, when the DERs are vulnerable to overload, a piece-wise linear droop characteristic is adopted.

The performance of the droop controller considering the voltage regulator and the filter dynamics is investigated by eigenvalue analysis. The analysis verifies the fast dynamic response and small-signal stability of the method. The method is then applied to the CIGRE benchmark microgrid and both step load change and islanding scenarios are studied. The simulation results demonstrate a smooth dynamic response, which settles within two cycles after the disturbance. Moreover, the voltage is maintained within 96% to 104% of nominal value. The narrow range of voltage variations on one hand and the fixed frequency operation on the other hand, imply high quality of energy delivered to the consumers.

The proposed control method is analogous to the voltage droop method in DC microgrids [21], where the converters output voltages are drooped in accordance to the output current. However, the method is discriminated from the virtual output inductance [10] and virtual resistance [11] methods in AC microgrids, which utilizes P-E/Q-f droop characteristics for power sharing.

It is worthwhile to compare the proposed method with adaptive feed-forward compensation scheme [17] and gain scheduled decoupling control strategy [18]. Similar to those methods, the proposed method adds two voltage signals into the q and d reference voltages. The voltage signals in all three methods are obtained by multiplying q and d axis currents by a gain matrix. However, the injected voltage in [17] and [18] are transient signals, introduced to improve the transient performance and stability of the P-f/Q-E droop controllers. On the other hand, the injected voltages in this paper are droop signals, which include both steady-state and transient components.

There is more to explore about the proposed control method. One of the next steps is to investigate the effect of harmonic and unbalanced load currents on the controller performance. Another is applying necessary modifications so that the method can be used for non-dispatchable DERs. Nevertheless this paper has laid out a novel droop control strategy, which aims at improving the dynamic response and stability of microgrids by exploiting the intrinsic features of voltage source inverters.

VI. References

[1] A. Purvins, H. Wilkening, G. Fulli, E. Tzimas, G. Celli, S. Mocci, *et al.*, "A European supergrid for renewable energy: local impacts and far-reaching challenges," *Journal of Cleaner Production,* vol. 19, pp. 1909-1916, 11// 2011.

[2] J. M. Guerrero, M. Chandorkar, T. Lee, and P. C. Loh, "Advanced Control Architectures for Intelligent Microgrids ; Part I: Decentralized and Hierarchical Control," *Industrial Electronics, IEEE Transactions on,* vol. 60, pp. 1254-1262, 2013.

[3] M. Babazadeh and H. Karimi, "A Robust Two-Degree-of-Freedom Control Strategy for an Islanded Microgrid," *Power Delivery, IEEE Transactions on,* vol. 28, pp. 1339-1347, 2013.

[4] K. T. Tan, P. L. So, Y. C. Chu, and M. Z. Q. Chen, "Coordinated Control and Energy Management of Distributed Generation Inverters in a Microgrid," *Power Delivery, IEEE Transactions on,* vol. 28, pp. 704-713, 2013.

[5] M. B. Delghavi and A. Yazdani, "A Unified Control Strategy for Electronically Interfaced Distributed Energy Resources," *Power Delivery, IEEE Transactions on,* vol. 27, pp. 803-812, 2012.

[6] M. Prodanovic and T. C. Green, "High-Quality Power Generation Through Distributed Control of a Power Park Microgrid," *Industrial Electronics, IEEE Transactions on,* vol. 53, pp. 1471 -1482, oct. 2006.

[7] F. Katiraei, M. R. Iravani, and P. W. Lehn, "Small-signal dynamic model of a micro-grid including conventional and electronically interfaced distributed resources," *Generation, Transmission Distribution, IET,* vol. 1, pp. 369-378, 2007.

[8] A. Bidram and A. Davoudi, "Hierarchical Structure of Microgrids Control System," *Smart Grid, IEEE Transactions on,* vol. 3, pp. 1963-1976, 2012.

[9] K. De Brabandere, B. Bolsens, J. Van den Keybus, A. Woyte, J. Driesen, and R. Belmans, "A Voltage and Frequency Droop Control Method for Parallel Inverters," *Power Electronics, IEEE Transactions on,* vol. 22, pp. 1107-1115, 2007.

[10] L. Yun Wei and K. Ching-Nan, "An Accurate Power Control Strategy for Power-Electronics-Interfaced Distributed Generation Units Operating in a Low-Voltage Multibus Microgrid," *Power Electronics, IEEE Transactions on,* vol. 24, pp. 2977-2988, 2009.

[11] J. M. Guerrero, J. Matas, V. Luis Garcia de, M. Castilla, and J. Miret, "Decentralized Control for Parallel Operation of Distributed Generation Inverters Using Resistive Output Impedance," *Industrial Electronics, IEEE Transactions on,* vol. 54, pp. 994-1004, 2007.

[12] R. Majumder, A. Ghosh, G. Ledwich, and F. Zare, "Angle droop versus frequency droop in a voltage source converter based autonomous microgrid," in *Power & Energy Society General Meeting, 2009. PES '09. IEEE*, 2009, pp. 1-8.

[13] E. Rokrok and M. E. H. Golshan, "Adaptive voltage droop scheme for voltage source converters in an islanded multibus microgrid," *Generation, Transmission & Distribution, IET,* vol. 4, pp. 562-578, 2010.

[14] Y. A. R. I. Mohamed and E. F. El-Saadany, "Adaptive Decentralized Droop Controller to Preserve Power Sharing Stability of Paralleled Inverters in Distributed Generation Microgrids," *Power Electronics, IEEE Transactions on,* vol. 23, pp. 2806-2816, 2008.

[15] R. Majumder, B. Chaudhuri, A. Ghosh, R. Majumder, G. Ledwich, and F. Zare, "Improvement of Stability and Load Sharing in an Autonomous Microgrid Using Supplementary Droop Control Loop," *Power Systems, IEEE Transactions on,* vol. 25, pp. 796-808, 2010.

[16] S. M. Ashabani and Y. A. R. I. Mohamed, "General Interface for Power Management of Micro-Grids Using Nonlinear Cooperative Droop Control," *Power Systems, IEEE Transactions on,* vol. 28, pp. 2929-2941, 2013.

[17] M. B. Delghavi and A. Yazdani, "An Adaptive Feedforward Compensation for Stability Enhancement in Droop-Controlled Inverter-Based Microgrids," *Power Delivery, IEEE Transactions on,* vol. 26, pp. 1764-1773, 2011.

[18] A. Haddadi, A. Yazdani, G. Joos, and B. Boulet, "A Gain-Scheduled Decoupling Control Strategy for Enhanced Transient Performance and Stability of an Islanded Active Distribution Network," *Power Delivery, IEEE Transactions on,* vol. 29, pp. 560-569, 2014.

[19] M. Bollen, Z. Jin, O. Samuelsson, and J. Bjornstedt, "Performance indicators for microgrids during grid-connected and island operation," in *PowerTech, 2009 IEEE Bucharest*, 2009, pp. 1-6.

[20] H. N. Papathanassiou S, Strunz K., "A benchmark low voltage microgrid network", CIGRE symposium on power systems with dispersed generation, 2005, p. 1–8.

[21] P. Karlsson and J. Svensson, "DC bus voltage control for a distributed power system," *Power Electronics, IEEE Transactions on,* vol. 18, pp. 1405-1412, 2003.

Mohammad S. Golsorkhi (S'13) received his B.Sc. (Hons.) and M.Sc. (Hons.) in electrical engineering from Isfahan University of Technology, Iran and Tehran Poly-technique, Iran, in 2009 and 2012, respectively. He is currently perusing the Ph.D. degree in The University of Sydney, Australia. His research interests include control of microgrids, renewable energy resources and power electronics.

Dylan Dah-Chuan Lu (S'00 – M'04 – SM'09) received his B.Eng. (Hons.) and Ph.D. degrees in Electronic and Information Engineering from The Hong Kong Polytechnic University, Hong Kong, in 1999 and 2004 respectively. In 2003, he joined PowereLab Ltd. as a Senior Design Engineer. His major responsibilities include project development and management, circuit design, and contribution of research in the area of power electronics. In 2006, he joined the School of Electrical and Information Engineering, The University of Sydney, Australia, where he is currently a Senior Lecturer. From July 2013 to December 2013, he was with the University of Hong Kong as a visiting Associate Professor. He presently serves as an Associate Editor of the International Journal of Electronics. He is an author/co-author of over 100 papers in the areas of power electronics and engineering education. He has two patents on efficient power conversion. His current research interests include power electronics circuits and control for efficient power conversion, lighting, renewable electrical energy systems, microgrid, motor drive and power quality improvement, and engineering education.
Dr. Lu received the Dean's Research Award in 2011 and is also a member of the Institute of Engineers Australia.